13th ewtec 2019 Proceedings of the 13th European Wave and Tidal Energy Conference 1-6 Sept 2019, Naples, Italy

The prediction of high turbulence lift and drag characteristics for use with marine turbine modelling

Matt Edmunds, Ross Gwenter, Alison J. Williams, and Ian Masters

***Abstract*—Analytical and computational tools such as Blade Element Momentum Theory (BEMT) and Blade Element Computational Fluid Dynamics (BE-CFD) rely on input data such as the lift and drag characteristics of the rotor foils. Thus it is important to use accurate input data to provide confidence in the results of such tools. For a given foil section profile, the lift and drag characteristics change with differing flow conditions, i.e. differing levels of turbulence and non smooth foils. This work investigates these issues and looks for trends in the data using CFD to simulate this phenomena.**

The CFD can predict the lift and drag characteristics of a foil with a good level of accuracy. The baseline CFD results correlate well with the experimental data. The change in performance observed in the presented cases is relatively small, however they have a significant effect on the overall forces when considering the application and fluid medium. Continuing this study with higher levels of turbulence and surface roughness would provide invaluable insight into the possibly nonlinear behaviour of lift and drag when these conditions change. An application of these characteristics on an example turbine will provide better understanding of the magnitude of the change in performance.

***Index Terms*—Enter at least three key words or phrases in alphabetical order, separated by commas.**

I. Introduction

ANALYTICAL and computational tools such as Blade Element Momentum Theory (BEMT) [1] [2] and Blade Element Computational Fluid Dynamics (BE-CFD) [3] are useful in predicting the performance of horizontal axis tidal turbines. In the case of BE-CFD, the downstream wake and downstream turbine interactions can also be predicted. However these tools rely on input data such as the lift and drag characteristics of the rotor foils. Thus it is important to use accurate input data to provide confidence in the results of such tools. The lift and drag characteristics of a given foil section profile changes with differing flow conditions. This can in part be captured using Reynolds number interpretations of the flow conditions, and matching that with the appropriately characterised lift and drag data. However, differing levels of turbulence can also significantly effect the foil section performance, particularly in stall conditions. Traditionally experiments examining the lift and drag characteristics of foil sections are intentionally run with minimal turbulence effects. This produces idealised or optimal lift and drag profiles. This is not ideal for deployed or flume based predictions of horizontal axis tidal turbines. Using lift and drag data that does not correctly represent the target environment can negatively influence predictive tools which rely on such data. This work investigates these issues and looks for trends in the data using CFD to simulate this phenomena, see fig 1.

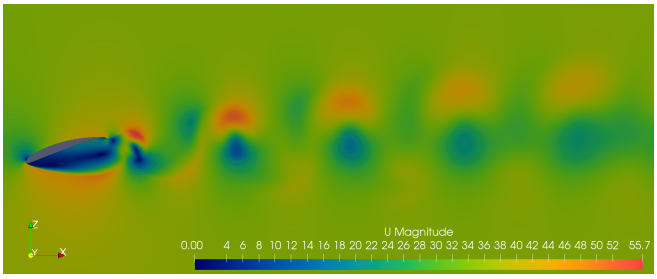

Fig. 1. SG6043 Aerofoil set at -18 degrees angle of attack, and colour mapped to velocity magnitude. The visualisation shows a stalled condition at Re=500,000 and thus vortex street set of velocity fluctuations resulting from oscillating flow separation.

II. Background to Aerofoil Prediction

The prediction of aerofoil characteristics such as lift and drag, with a focus of predicting aircraft performance, is a well studied subject [4]. There is much data available for a range of aerofoils both experimental [5], and analytical [6] [7]. However, in most cases the focus is on high Reynolds number predictions of lift and drag within the pre stall set of angles of attack. There is often data showing the change in performance due to the addition of a defined rough surface simulating wing icing effects [5]. In addition, the effects of turbulence

Paper ID number: 1620- Conference track: Tidal Hydrodynamic Modelling

The Author(s) acknowledge(s) the financial support provided by the Welsh Government and Higher Education Funding Council for Wales through the Sêr Cymru National Research Network for Low Carbon, Energy and Environment. (C001822). The work was also supported by the EPSRC funded "Extension of UKCMER Core Research, Industry and International Engagement" project (EP/M014738/1), and the SURFTEC SuperGen grand challenge project, funded under EPSRC grant (EP/N02057X/1).

M. Edmunds is with the Marine Energy Research Group Energy Safety Research Institute (ESRI) College of Engineering Swansea University Bay Campus Fabian Way Crymlyn Burrows Swansea SA18EN Wales U.K. (e-mail: m.edmunds@swansea.ac.uk).

R. Gwenter is with the Marine Energy Research Group Energy Safety Research Institute (ESRI) College of Engineering Swansea University Bay Campus Fabian Way Crymlyn Burrows Swansea SA18EN Wales U.K. (e-mail: 881656@swansea.ac.uk).

A. J Williams is with the Marine Energy Research Group Energy Safety Research Institute (ESRI) College of Engineering Swansea University Bay Campus Fabian Way Crymlyn Burrows Swansea SA18EN Wales U.K. (e-mail: alison.j.williams@swansea.ac.uk).

I.Masters is with the Marine Energy Research Group Energy Safety Research Institute (ESRI) College of Engineering Swansea University Bay Campus Fabian Way Crymlyn Burrows Swansea SA18EN Wales U.K. (e-mail: i.masters@swansea.ac.uk).

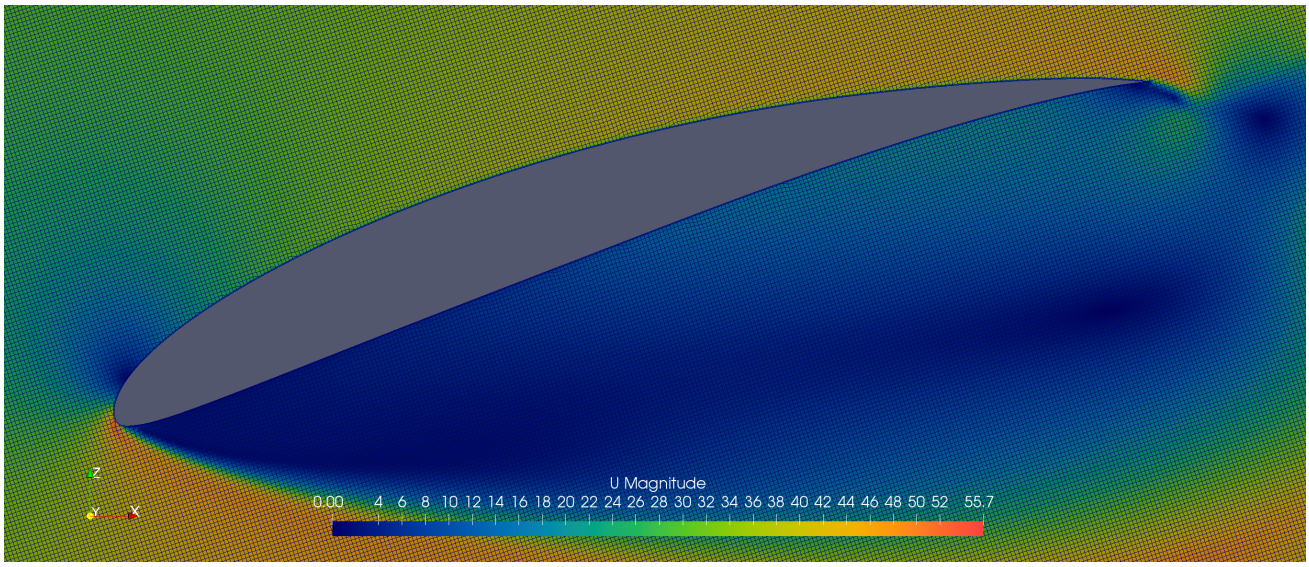

Fig. 2. SG6043 foil profile; thickness 10%, camber 5.5%. This image of the foil is set at and angle of attack of -18 degrees, and free stream velocity is 35m/s.

intensity (TI) on performance is neglected in these studies. This is due to the turbulent fluctuations being small relative to the speed of the aircraft, and thus implies small levels of turbulence intensity.

In contrast with the aero environment, lift and drag characteristics in the marine environment are usually a function of; high turbulence intensity, often operating at lower Reynolds numbers (particularly at lab scale), and significant levels of surface roughness possibly due to fouling. This makes the use of existing experimental data from the aero environment too optimal for the accurate prediction of marine environment case studies. In addition to these issues, analytical approaches for predicting lift and drag characteristics generally have problems with the accurate prediction of stall. This is exacerbated at lower Reynolds numbers, and the general inability to predict turbulent and surface roughness effects [8].

For use with models that predict Horizontal Axis Tidal Turbine performance, such as BEMT [9] and BEM-CFD [3], coefficients of lift and drag (Cl and Cd) at the required operating conditions are assembled and inputted into the given model. This model will perform calculations using this data in conjunction with geometric aspects of the foil, i.e. chord, twist and angle of attack, to compute the local forces:

$$LiftForce = 0.5\ \rho\ U^2\ c\ Cl(\alpha) \tag{1}$$

$$DragForce = 0.5\ \rho\ U^2\ c\ Cd(\alpha) \tag{2}$$

Where ρ is fluid density $[kg/m^3]$, U is fluid velocity $[m/s]$, c is chord length $[m]$, α is the angle of attack, and Cl/Cd are coefficients of lift and drag respectively.

Within the aforementioned models U is to be determined based on some pre defined set of initial/boundary conditions. These computations are thus directly influenced by the results of equations 1 and 2. With this in mind it is thus important to provide accurate inputs to these types of model, and thus it is better to describe Cl and Cd in terms of:

$$LiftForce = 0.5\ \rho\ U^2\ c\ Cl(\alpha, TI, Re, Ro) \tag{3}$$

$$DragForce = 0.5\ \rho\ U^2\ c\ Cd(\alpha, TI, Re, Ro) \tag{4}$$

Where TI is turbulence intensity, Re is Reynolds number, and Ro is foil surface roughness.

III. The Study of the SG6043 Aerofoil

This study outlines the change in lift and drag characteristics as a result of increasing turbulence with respect to a given fluid medium and free stream velocity, i.e. Reynolds number dependence. An example foil (SG6043) is studied with respect to experimental results conducted by Giguere and Selig [10]. This foil design is established to provide better performance characteristics at lower relative velocities and improve stall performance. Thus this foil has superior operation at lower Reynolds numbers and higher angles of attack.

CFD is used to determine a baseline Cl and Cd with respect to the angle of attack, and the results are compared and contrasted with the experimental result by [10]. For this study OpenFoam is utilised as the CFD software of choice [11]. Once the baseline result is established, further CFD simulations are conducted set with higher levels of turbulence intensity. The results are then contrasted with the baseline data to establish trends in the deviation of lift and drag with respect to turbulent intensity.

A. Mesh Configuration

The initial mesh is constructed using the blockMesh utility representing a domain size of 30 metres by 30 metres. This domain is then subdivided into 130 cells by 130 cells. Once this is complete the mesh is then refined using the snappyHexMesh utility and an 'stl' file representing the aerofoil geometry. The chord length of the aerofoil is set at 1 metre. A refinement

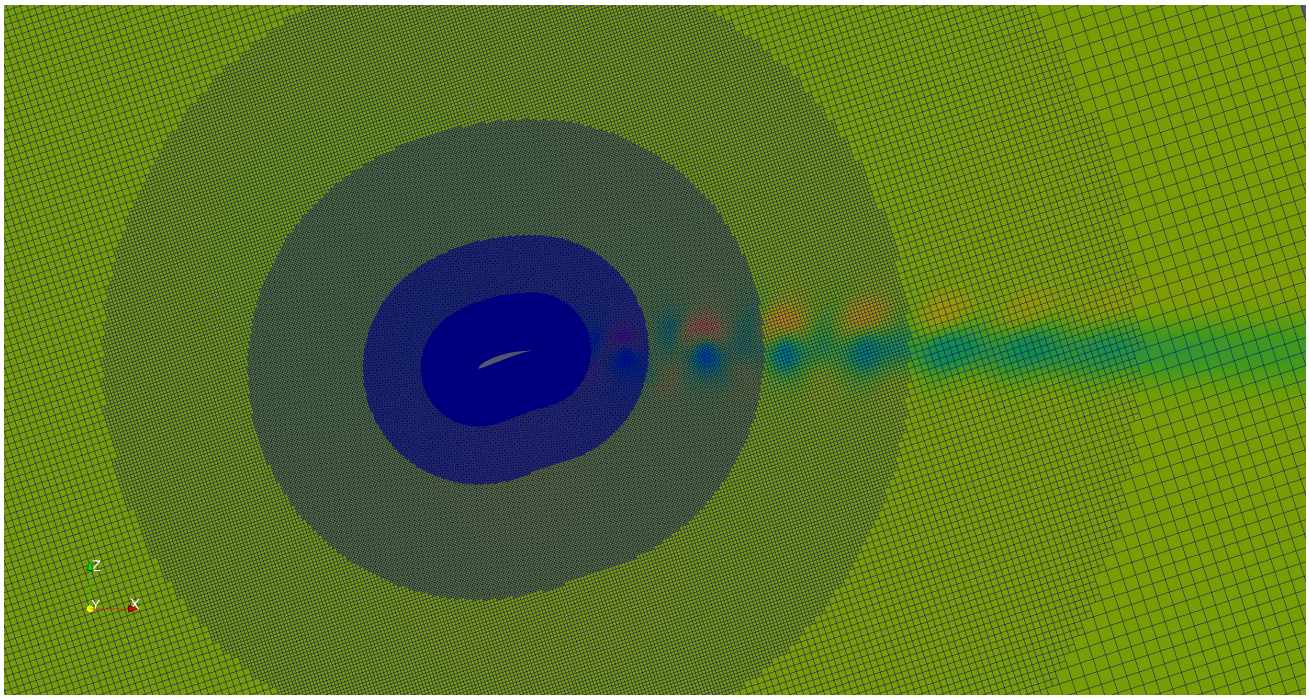

Fig. 3. SG6043 foil profile; thickness 10%, camber 5.5%. This image of the foil is set at and angle of attack of -18 degrees, and free stream velocity is 35m/s. This image shows the variation in mesh density, becoming coarser towards the outer domain boundary.

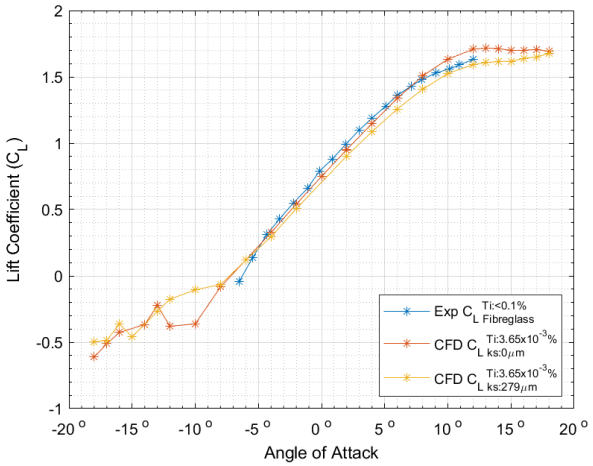

Fig. 4. SG6043 experimental, no roughness and rough surface CFD cases at <1% TI. Coefficient of lift is plotted against angle of attack at Re=500,000.

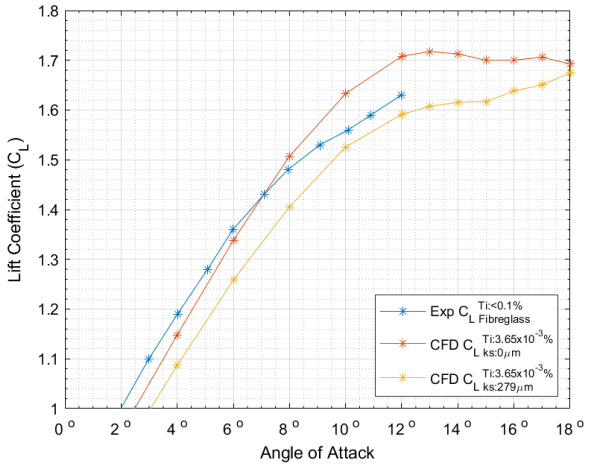

Fig. 5. SG6043 experimental, no roughness and rough surface CFD cases at <1% TI. Coefficient of lift is plotted against angle of attack at Re=500,000. Close up of the stall region.

level of 6 is set for up to 0.5 metres from the foil, level 5 up to 1 metre, level 4 up to 2 metres, level 3 up to 4 metres, level 2 up to a radius of 7 metres, and level 1 up to a radius of 11 metres, see fig 2 and fig 3. A boundary layer is constructed against the foil with a cell height of 0.001 metres.

B. Boundary and Initial Conditions

The model is set with a free stream velocity of 35 metres per second, and a fluid kinematic viscosity of 0.000014 metres squared per second. The 'kOmegaSST' RAS turbulence model is used to support the prediction of turbulent viscosity. Turbulent kinetic energy is set with a selection of values for the different turbulence levels studied: k = 0.00000049 for TI < 1%, k = 1.65 for TI = 3%, and k = 4.59 for TI = 5%.

The outer domain boundary is set with an 'inout' or free stream boundary condition aligned with the x axis direction, see fig 3. Different angles of attack are specified by rotating the mesh by the required angle to set the required flow direction. The aerofoil itself is set with; a fixed value of zero for velocity, zero gradient for pressure, and wall functions are specified for turbulent kinetic energy and turbulent viscosity.

The 'pimpleFoam' transient incompressible pressure velocity coupled solver is used to resolve the discretised domain. An adjustable time step is specified with a max Courant number of 0.9 as the constraint. The aerofoil forces and coefficients are calculated and

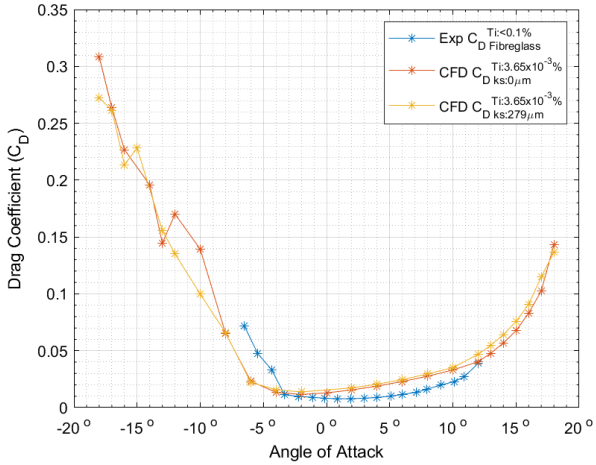

Fig. 6. SG6043 experimental, no roughness and rough surface CFD cases at <1% TI. Coefficient of drag is plotted against angle of attack at Re=500,000.

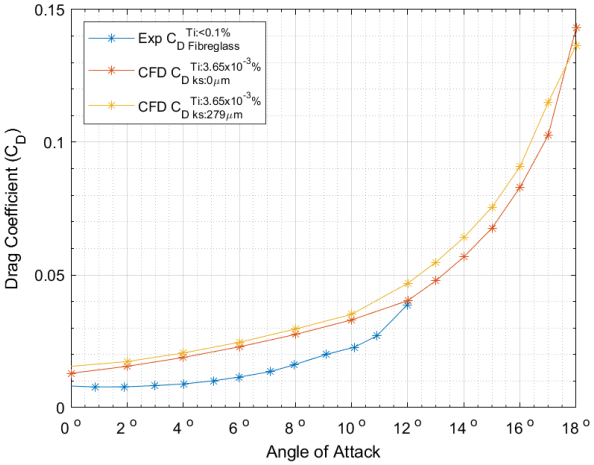

Fig. 8. SG6043 experimental, no roughness and rough surface CFD cases at <1% TI. Coefficient of drag is plotted against angle of attack at Re=500,000. Close up of the stall region.

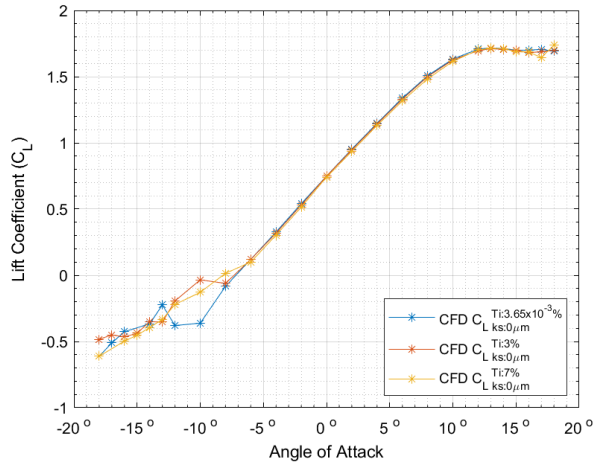

Fig. 7. SG6043 no roughness CFD cases at <1% TI, TI = 3% and TI = 7%. Coefficient of lift is plotted against angle of attack at Re=500,000.

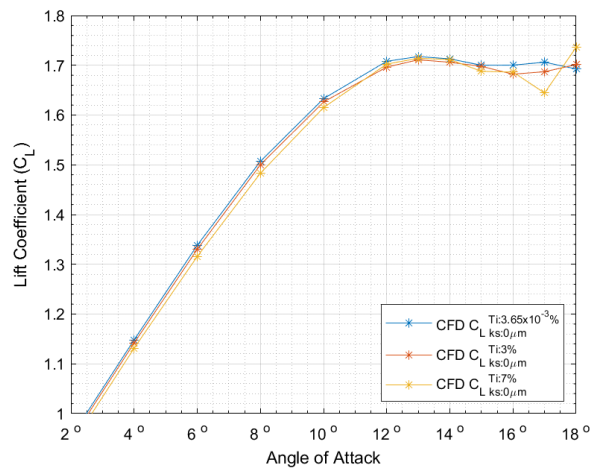

Fig. 9. SG6043 no roughness CFD cases at <1% TI, TI = 3% and TI = 7%. Coefficient of lift is plotted against angle of attack at Re=500,000. Close up of the stall region.

stored for each computed time step.

The pressure field is resolved using the 'GAMG' multilevel cell agglomeration algorithm, while the velocity field is resolved using the 'PBiCGStab' algorithm. The Pimple algorithm is set with residual tolerances of 0.00001, and solves with 4 inner correctors and 50 outer correctors.

IV. Results

In this section lift and drag characteristics for the SG6043 foil are presented for a range of turbulent conditions. These results are compared and contrasted with the experimental results presented in [10] and trends between the different turbulent cases are discussed.

C. Baseline Results

In this subsection the low turbulence case results are presented, i.e. TI < 1%. These results are directly compared with the experimental results from [10]. Fig 4 and 6 demonstrate the coefficient of lift and drag plotted against angle of attack respectively. Good agreement can be observed between the experimental results for lift and drag and the CFD results for the low turbulence case i.e <1%. It can be seen that stalling occurs at a slightly higher angle of attack with the CFD result. The experimental aerofoil is likely manufactured with a level of surface roughness (although very small i.e. machined finish) which is likely to influence the stall characteristic of the foil. However, as the CFD assumes a perfect smooth surface there is a small offset (with reference to angle of attack) in the development of stall. With this caveat to the agreement likely to propagate through the remaining CFD studies, it is important to consider the trends in such cases.

D. Increasing Surface Roughness

With reference to figs 4 and 5 the general trend is a reduction in lift for a given angle of attack when comparing the rough surface CFD curve to the smooth surface CFD curve. The trend is increasing with increasing angle of attack, however in the fully stalled regions, i.e. negative and positive stall, the lift

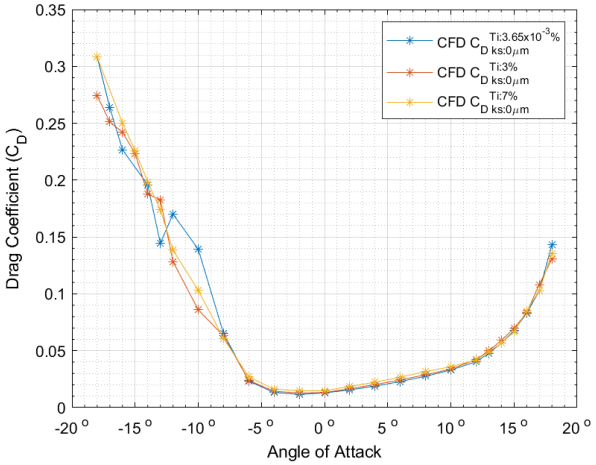

Fig. 10. SG6043 no roughness CFD cases at <1% TI, TI = 3% and TI = 7%. Coefficient of drag is plotted against angle of attack at Re=500,000.

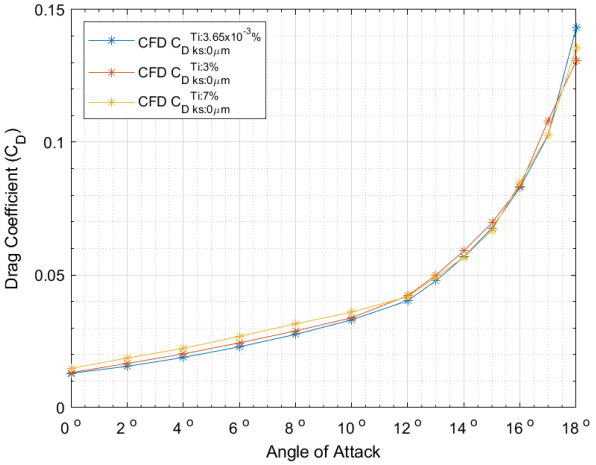

Fig. 12. SG6043 no roughness CFD cases at <1% TI, TI = 3% and TI = 7%. Coefficient of drag is plotted against angle of attack at Re=500,000. Close up of the stall region.

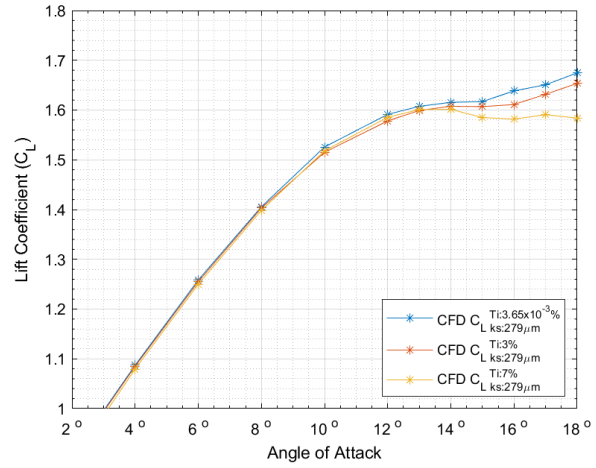

Fig. 11. SG6043 rough surface CFD cases at <1% TI, TI = 3% and TI = 7%. Coefficient of lift is plotted against angle of attack at Re=500,000. Close up of the stall region.

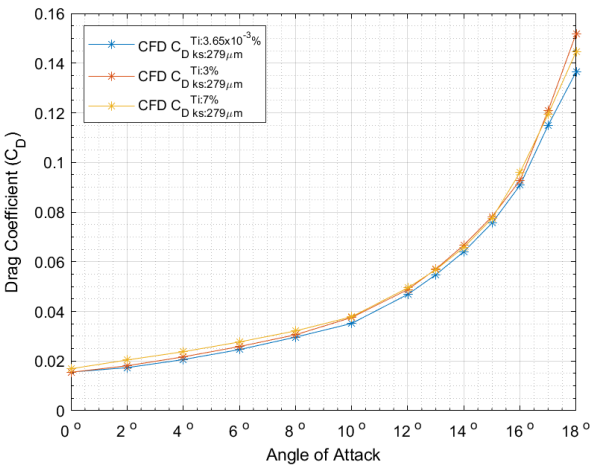

Fig. 13. SG6043 rough surface CFD cases at <1% TI, TI = 3% and TI = 7%. Coefficient of drag is plotted against angle of attack at Re=500,000. Close up of the stall region.

characteristics head towards convergence. The lower lift characteristic of the rough foil is attributed to the separation point of the flow on the top surface of the foil starting and moving upstream at lower angles of attack. This occurs when the boundary layer thickness increases, due to the simulated rough surface, allowing for easier detachment of the fluid flow from the upper surface of the foil.

Figs 6 and 8 show the results of drag plotted against angle of attack. The general trend is an increase in drag for the rough surface foil as compared to the smooth. It can be seen that the drag difference increases away from zero angle of attack until full stall is reached. This is in line with the trends observed in the lift curves discussed above, and is attributed again to the increased boundary layer thickness inducing additional drag.

E. Increasing Turbulence Intensity

Figs 7 and 9 show lift plotted against angle of attack for a range of turbulent intensities (TI). The low turbulence case, i.e. <1% TI, produces the highest lift. The general trend when increasing the turbulence intensity is a reduction in lift. However, this trend changes in the stall region where the higher turbulence case starts to increase lift during the onset of full stall. The difference between cases appears small, however it can have have a significant effect on the overall forces when considering the application and fluid medium.

Similar trends can be observed in figs 10 and 12, i.e. the drag increases with increasing turbulence intensity. This again changes in the stall region where the drag decreases relative to the lower TI cases.

These characteristics are again attributed to changes in the boundary layer region. In the case of higher turbulence, the boundary layer is affected by the change in turbulence levels similar to the rough surface effect.

F. Combining Turbulence and Roughness

The final set of results show lift and drag curves simulated with surface roughness combined with increasing levels of turbulence, see figs 11 and 13. Similar lift and drag trends are observed as discussed in the

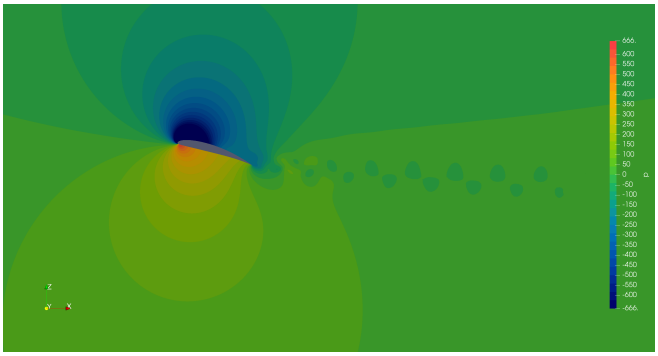

Fig. 14. SG6043 foil profile; thickness 10%, camber 5.5%. This image of the foil is set at and angle of attack of -17 degrees, and free stream velocity is 35m/s. This image shows the pressure fluctuations as a result of vortex shedding with turbulence set to <1% TI.

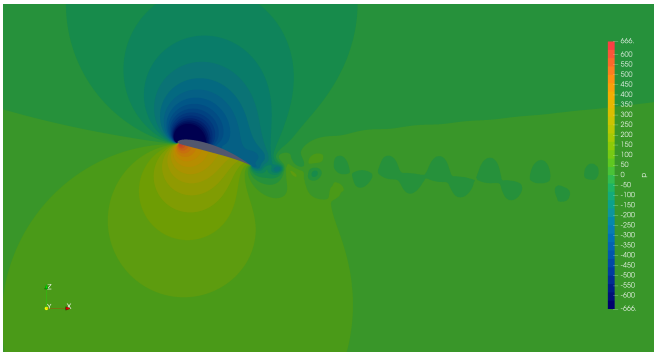

Fig. 15. SG6043 foil profile; thickness 10%, camber 5.5%. This image of the foil is set at and angle of attack of -17 degrees, and free stream velocity is 35m/s. This image shows the pressure fluctuations as a result of vortex shedding with turbulence set to 7% TI.

previous subsections. As the level of turbulence intensity increases, the lift reduces while drag increases. The reduction in lift and increase in drag are compounded when considering both surface roughness and increasing turbulence together.

G. Stall Fluctuations

As can be seen in figs 1, 2 and 3, vortex streets are shed from the foil during stall. These fluctuations in velocity, and thus pressure, generate a variation in lift and drag at a given angle of attack. These fluctuations increase in intensity as the turbulence/roughness is increased, see figs 14 and 15.

V. Conclusions

It can be seen that CFD can predict the lift and drag characteristics of a foil with a good level of accuracy. The baseline CFD results correlate well with the experimental data. This is an important result as it provides confidence in the method, and thus any modification of the CFD baseline case.

The increasing levels of turbulence negatively affects the performance of the foil, however at higher levels of stall there appears to be a smaller post stall drop in performance. This is accentuated with the inclusion of rough surface characteristics to the foil surface.

The stall related fluctuations increase with angle of attack into the fully stalled region. These fluctuations increase in energy as the roughness/level of turbulence increases.

The change in performance observed in the presented cases is relatively small, however they have a significant effect on the overall forces when considering the application and fluid medium. The change in performance appears nonliniar as turbulence is increased, this effect may carry over to the application of surface roughness. For example an application of these effects to a horizontal axis marine turbine may see as much as 5% drop in performance [2].

Continuing this study with higher levels of turbulence and surface roughness would provide invaluable insight into the possibly nonlinear behaviour of lift and drag when these conditions change. Also of significant interest is a full study of the magnitude and deviation of the fluctuations through the range of angles of attack with differing levels turbulence/roughness. An application of these characteristics on an example turbine will provide better understanding of the magnitude of the change in performance.

References

[1] J. Chapman, I. Masters, M. Togneri, and J. Orme, "The buhl correction factor applied to high induction conditions for tidal stream turbines," *Renewable Energy*, vol. 60, pp. 472–480, 2013.

[2] I. Masters, A. J. Williams, T. N. Croft, M. Togneri, M. Edmunds, E. Zangiabadi, I. Fairley, and H. Karunarathna, "A comparison of numerical modelling techniques for tidal stream turbine analysis," *Energies*, vol. 8, no. 8, pp. 7833–7853, 2015.

[3] M. Edmunds, A. J. Williams, I. Masters, and T. N. Croft, "An enhanced disk averaged CFD model for the simulation of horizontal axis tidal turbines," *Renewable Energy*, vol. 101, pp. 67 – 81, 2017. [Online]. Available: http://www.sciencedirect.com/science/article/pii/S096014811630708X

[4] J. Anderson, *Fundamentals of Aerodynamics*, ser. Anderson series. McGraw-Hill Education, 2010, no. 5. [Online]. Available: http://books.google.co.uk/books?id=xwY8PgAACAAJ

[5] I. Abbott and A. Von Doenhoff, *Theory of Wing Sections, Including a Summary of Airfoil Data*, ser. Dover Books on Aeronautical Engineering Series. Dover Publications, 1959, no. 1.

[6] Airfoil Tools, "Airfoil Tools," http://airfoiltools.com/, Retrieved: February 2019.

[7] Martin Hepperle, "JavaFoil," https://www.mh-aerotools.de/airfoils/javafoil.htm, Retrieved: August 2018.

[8] R. Malki, I. Masters, A. J. Williams, and T. Nick Croft, "Planning tidal stream turbine array layouts using a coupled blade element momentum–computational fluid dynamics model," *Renewable Energy*, vol. 63, pp. 46–54, 2014.

[9] M. Togneri, I. Masters, and J. Orme, "Incorporating turbulent inflow conditions in a blade element momentum model of tidal stream turbines," in *21st (2011) International Offshore and Polar Engineering Conference (ISOPE)*, 2011.

[10] M. Selig, "New airfoils for small horizontal axis wind turbines," *Urbana*, vol. 51, pp. 61 801–2935, 1998.

[11] H. G. Weller, G. Tabor, H. Jasak, and C. Fureby, "A tensorial approach to computational continuum mechanics using object-oriented techniques," *Computers in Physics*, vol. 12, no. 6, pp. 620–631, 1998.